2011 International Nuclear Atlantic Conference - INAC 2011
Belo Horizonte,MG, Brazil, October 24-28, 2011
ASSOCIAÇÃO BRASILEIRA DE ENERGIA NUCLEAR - ABEN
ISBN: **978-85-99141-04-5**

^{234}Th AS A TRACER OF ORGANIC CARBON EXPORT IN BRANSFIELD STRAIT, ANTARTIC

Joselene de Oliveira[1], Lúcia Helena Vieira[1], Elisabete de Santis Braga[2], Celina Lopes Duarte[3]

[1] Laboratório de Radiometria Ambiental
Gerência de Metrologia das Radiações
Instituto de Pesquisas Energéticas e Nucleares (IPEN / CNEN - SP)
Av. Professor Lineu Prestes 2242
05508-000 São Paulo, SP
jolivei@ipen.br

[2] Instituto Oceanográfico da Universidade de São Paulo
Praça do Oceanográfico, 191 Cidade Universitária
05508-900 São Paulo, SP
edsbraga@usp.br

[3] Centro de Tecnologia das Radiações
Instituto de Pesquisas Energéticas e Nucleares (IPEN / CNEN - SP)
Av. Professor Lineu Prestes 2242
05508-000 São Paulo, SP
clduarte@ipen.br

ABSTRACT

The element thorium has multiple isotopes that have emerged collectively as a powerful set of tracers for particle associated processes in the oceans. The production of ^{234}Th from ^{238}U, coupled with the conservative behavior of ^{238}U in seawater, makes the source of ^{234}Th easy to characterize. Because of its very particle reactive behavior, ^{234}Th is removed from a parcel of water in only two ways, through decay and through particle flux. Therefore, a steady-state 1D activity balance can be used to calculate its flux. This work presents results of a collaborative research on organic carbon fluxes distribution in the Bransfield Strait. Macro-nutrients, micronutrients and chlorophyll-a distributions were used to examine the pathway sources. ^{234}Th was used as a tracer of organic carbon fluxes distribution in the Bransfield Strait in order to evaluate its influence in the CO_2 drawdown, since POC export via sinking particles is the primary mechanism of carbon sequestration in the Southern Ocean. Fluxes up to 15274 dmp m^{-2} d^{-1} were estimated, the highest value observed in Station 09 at 794 m depth. POC exported fluxes derived from the disequilibrium ^{234}Th/ ^{238}U model varied from 0.6 to 16000 mmol C m^{-2} d^{-1}.

1. INTRODUCTION

Although estimates vary, about 1/3 of the CO_2 that is released to the atmosphere by human activities (e.g., deforestation and burning fossil fuels) is taken up by the ocean. Highlighted by the major scope of global climate changes, the extent to which this carbon is incorporated into biological production in the ocean has become an area of intense interest.

The Southern Ocean is the largest oceanic area with a high inventory of macro-nutrients available in surface waters and relatively low phytoplankton chlorophyll. This region is significantly important for intermediate and deep water masses formation and very favorable

for CO_2 sequestration from the atmosphere to the ocean interior via biological pump [1-5]. An important feature of island systems in the high-nutrient low-chlorophyll (HNLC) waters of the Southern Ocean is the elevated levels of productivity observed around them during the austral summer [1, 2]. This island effect has been hypothesized to be due to iron release from these islands and associated shelf systems into the surrounding waters, thus allowing primary production to occur in this HNLC zone.

It has long been known that a certain fraction of the production of marine organic matter escapes the euphotic zone (approximately upper 100 m) and sinks to depth, either as fecal pellets or as sinking aggregates termed "marine snow" [3]. This sinking or export flux of POC removes C from the surface water and adds it to deep oceans, where some of it is decomposed and a small fraction reaches the bottom. The magnitude of the POC export has been estimated from nutrient balances in the euphotic zone, such that the production supported by the supply of "new" nutrients via upwelling, for example (called new production), is balanced by the export of POC. Other approaches for estimating POC export include the use of sediment traps that collect sinking particles, although these are often subject to significant problems such as biases associated with the flow of water over the trap face [6].

The natural U and Th decay series present several nuclides with half-lives varying from fractions of a second to a few years. In these series there are nuclides with half-lives that make them useful in tracing a variety of oceanic processes that occur on short time scales. This group includes isotopes of thorium: ^{234}Th (half-life = 24.1 d), ^{227}Th (18.6 d), ^{228}Th (1.9 y), radium: ^{224}Ra (3.64 d), ^{223}Ra (11.1 d), radon: ^{222}Rn (3.8 d) and polonium: ^{210}Po (138 d). Of these, the Th isotopes and ^{210}Po are particle-reactive, while radium isotopes and radon tend to remain in solution. As a consequence, Th and Po are useful in quantifying the rate of scavenging from solution onto particles and processes governing the dynamics of particles in the ocean, while Ra and Rn are appropriate tracers for fluid processes such as advection and diffusion [6].

Processes that fractionate nuclides within a chain produce parent-daughter disequilibrium; the return to equilibrium then allows quantification of time. Because of the prescribed decay behaviour, U-series disequilibria can be used for geochronology or for examining the rates and time scales of any dynamic processes which induces fractionation. In many cases, the direction of disequilibrium (activity ratios above or below one) provides a powerful means of tracing specific processes. The key to the utility of the U-series is that several natural processes are capable of disrupting the state of equilibrium. Two types of mechanisms need to be distinguished here. Firstly, each element has distinct chemical properties and thus, the U-series nuclides can become fractionated during processes that discriminate chemical behaviour: phase change, partial melting, crystallization, partitioning, dissolution, adsorption, degassing, oxidation/reduction and complexation. Secondly, fractionation can also take place as a result of radioactive decay, especially in the low-temperature environment, and these effects are generally described as recoil effects.

The application of Th isotopes and ^{210}Po have in common the fact that each is produced by a longer lived parent which is stably dissolved or tends to remain in solution longer than its progeny. ^{234}Th is considered a useful tracer of oceanic biogeochemical processes occurring over time scales of days to weeks. ^{234}Th is a naturally occurring radionuclide constantly produced in seawater by its soluble parent ^{238}U. Due to its high particle reactivity and

relatively short half-life ($t_{1/2}$ = 24.1 days), ^{234}Th is commonly used as a proxy to estimate POC export from the upper oceanic water column. This export is usually assessed by quantifying total ^{234}Th deficits with respect to its conservative parent nuclide ^{238}U in seawater.

^{234}Th short half-life makes it sensitive to seasonal changes in the processes of POC production and export. Indeed, this is one of the most significant applications of ^{234}Th/^{238}U disequilibrium within the past 20 years. The approach builds on the observations of ^{234}Th deficiencies in the upper ocean described above and argues that such deficiencies are created by the scavenging of ^{234}Th onto biogenic particles and the sinking of such particles out of the euphotic zone. Some investigations explicitly showed that the pattern of ^{234}Th/^{238}U disequilibrium in the upper 100 m of the North Pacific gyre and the California Coastal Current was linked to profiles of nutrients and dissolved O_2, such that production and cycling of organic matter were causing the ^{234}Th disequilibrium [6].

The preliminary isotopic approach proposed that if the residence time of Th with respect to sinking could be applied to the standing crop of POC in the euphotic zone, as seems reasonable if sinking POC is responsible for ^{234}Th removal, then the sinking flux of POC could be calculated. This flux was firstly equated to the new production and argued that ^{234}Th disequilibrium would be a useful approach to determining new production in the oceans. In the following studies, however, residence times of both POC and particulate ^{234}Th in the eastern Equatorial Pacific estimated through this method showed different results [6]. In part the disparity was attributed to the way the particulate ^{234}Th residence time was calculated, but because the chemistries of C and Th are substantially different with respect to their incorporation and cycling in organic matter, it is likely that their residence times would be different in the euphotic zone.

The better agreement is obtained from a one-box model approach, in which the particulate residence time is calculated as the difference between the residence times of total Th and dissolved Th. However, Buesseler *et al.* [2] showed that there is abundant evidence to support the notion that residence times of POC and Th are different in the euphotic zone. These authors proposed a method to circumvent these difficulties in comparing residence times. They suggested that the deficiency in total ^{234}Th with respect to ^{238}U indicates a flux of ^{234}Th in association with particles sinking out the euphotic zone. In this case, if POC (or particulate organic nitrogen, PON)/ ^{234}Th ratio of these sinking particles are known, a POC (or PON) flux can be assessed.

This paper presents results of a collaborative research on organic carbon fluxes distribution in the Bransfield Strait in order to evaluate its influence in the CO_2 drawdown. Macro-nutrients, micro-nutrients and chlorophyll-a distributions are used to examine the sources and its role on primary production. ^{234}Th was used as a tracer of particle flux in the upper ocean, since POC export via sinking particles is the primary mechanism of carbon sequestration in the Southern Ocean.

2. MATERIAL AND METHODS

2.1. Study site and sampling protocols

The Bransfield Strait, situated west of the Antartic Peninsula, has been considered as a highly productive region for all trophic levels from primary production, to zooplacton aggregations, especially krill, to birds and mammals. The bottom topography of the Bransfield Strait consists of a central basin deeper than 1000 m that is bounded to the northwest by the steep continental margin of the South Shetland Islands, to the southeast by the Antartic Peninsula and to the southwest, referred to as the Gerlache Strait, by shallow shelves and islands. The shelf slope waters around the South Shetland Islands consist of the water strong influenced by local processes of heating and freshwater runoff referred to as the Shelf Slope Water, and the intrusion water from the Antartic Circumpolar Current deep water which intrudes into the Bransfield Strait from the deep through between Brabant and Smith Islands and remains near the South Shetland Islands. At the shelf slope, a western boundary current, the Bransfield Current, was revealed from the relative geostrophic circulation estimates based on hydrographic data. This current determines the water export from the Bransfield Strait through the shelf slope of the South Shetland Islands and transport of nutrients, metals and biota [7].

For the purposes of this research work, seawater samples were collected between 22nd November and 23th December 2007 (OPERANTAR XXVI) onboard the RV Ary Rongel, from Brazilian Navy. The sampling cruise covered an area located between latitude 63°S and longitude 54°W (**Fig. 1**).

Vertical profiles of total ^{234}Th were collected from 2-liter samples taken from Go-flow or Niskin bottles deployed by rosette within the upper 1000 m on 12 separate casts. Within 1 h of collection, unfiltered 2-liter samples for total ^{234}Th determination were acidified to pH 2 with 6 ml of concentrated HNO_3. After shaking the samples vigorously, ^{229}Th was added as a yield monitor. The sample was shaken again and allowed to equilibrate for 12 h. After equilibration, the pH was adjusted to 8 with concentrated NH_4OH. Extraction of thorium from samples was accomplished by co-precipitation of thorium via MnO_2 precipitate formed by the addition of $KMnO_4$ and $MnCl_2$ solutions [8, 9]. Samples were shaken vigorously after the addition of each reagent and allowed to stand for 12 h followed by filtration onto 47 mm diameter glass fiber filters. Finally, the filtered MnO_2 precipitates were dried overnight and mounted under one layer of Mylar film and two layers of standard aluminum foil in preparation for beta counting. Analyses of total ^{234}Th activities were performed at the Environmental Radiometrics Laboratory of IPEN/CNEN-SP using a gas-flow low background proportional counter from EG&G Berthold, model LB 770, following methods described in Buesseler *et al.*, 2001 [8]. Initial beta counting for 6-24 h was followed by a final background count in the lab after decay of ^{234}Th for at least six half-lives. Initial count rates were typically 2-4 counts per minute (cpm) for total ^{234}Th and final count rates averaged 0.5 cpm relative to the detector backgrounds of 0.4-0.6 cpm. For total ^{234}Th samples, anion exchange chemistry was performed and recovery of our added ^{229}Th yield monitor was quantified by inductively coupled plasma-mass spectroscopy. Corrections were applied to ^{234}Th activity calculations on the basis of ^{229}Th recoveries. All data are decay corrected to the time of collection and reported with a propagated error that includes uncertainties associated

with counting, sample volumes and other calibration errors. Errors were typically ± 0.04 – 0.06 cpm L^{-1} on total ^{234}Th.

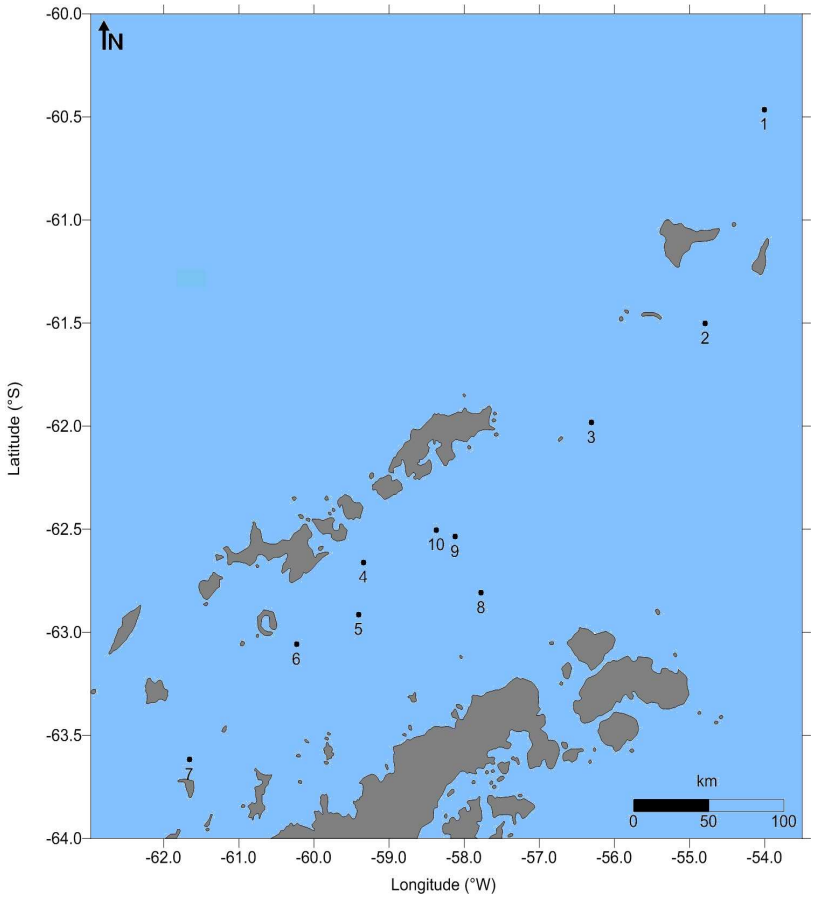

Figure 1. Location of oceanographic stations performed in the Bransfield Strait, Antartic, during the 2nd phase of OPERANTAR XXVI (2007).

Additional seawater samples were collected in sampled-rinsed polyethylene bottles, and filtered through HCl-washed Whatman GF/F filters immediately upon sample collection. Those samples were kept frozen until the return of the RV Ary Rongel to Brazil, where they were assayed in the chemical laboratory of the Oceanographic Institute of the University of São Paulo (Labnut) for nitrate, ammonia, silica and inorganic phosphate analyses following recommended procedures [10-12]. Aliquots for chlorophyll-a analysis (100 – 200 mL) were filtered onto 47 mm Whatman GF/F filters. These filters were extracted by 10 mL of 90% acetone during at least 24 h in dark before measurement using a fluorometric method. Three drops of 10% HCl were used to correct for phaeopigments. All samples were analyzed in duplicates.

Particulate organic carbon analyses were performed in the suspended material collected in GF/F filters following the filtration of 1000 mL of each seawater sample. The quantification

was carried out using gas chromatograph associated to mass spectrometry in a Shimadzu CGMS, model QP-5000, with a Head Space concentrator and He as a carrier gas [13]. These analyses were carried out at the Center of Radiation Technology of IPEN/CNEN-SP.

2.2. ^{234}Th derived particle export

^{234}Th is a naturally occurring particle-reactive radionuclide which has been commonly used to study particle scavenging in the upper ocean [2, 6, 8]. Since the half-life of ^{234}Th is 24.1 days, the disequilibrium between its soluble conservative parent ^{238}U and the measured ^{234}Th activity reflects the net rate of particle export from the upper ocean on time scales of days to weeks. In the surface ocean, both the formation of fresh particle surfaces (proportional to primary production) and the packaging of particles into sinking aggregates (export or new production) are reflected in the observed ^{234}Th distribution. The activity balance of ^{234}Th can be described by the following equation:

$$\frac{dA_{Th}}{dt} = A_U \lambda - A_{Th} \lambda - P + V \qquad (1)$$

Where dA_{Th}/dt is the change in the ^{234}Th activity with time, A_U is the ^{238}U activity (^{238}U in dpm L^{-1} is equal to 0.0686 x salinity [14]), A_{Th} is the total measured ^{234}Th activity, λ is the decay constant for ^{234}Th (0.0288 d^{-1}), P is the net removal flux of ^{234}Th on particles, and V is the sum of advective and diffusive terms. The magnitude of the export flux is most often driven by the extent of the ^{234}Th/^{238}U disequilibrium. Steady state is often assumed (dA_{Th}/dt = 0) and physical processes ignored. However, non steady state effects and physical processes can be substantial in some cases [15-17]. The use of non-steady state ^{234}Th formulations appears to be important during plankton blooms, when significant ^{234}Th removal can occur [18]. More commonly, however, steady-state models are sufficient [19]. Vertical advection, V in equation (1), has been shown to be significant in areas of intense upwelling, such as in the Equatorial Pacific and along the coast of the Arabian Sea during the SW Monsoon [16, 17]. In addition, horizontal ^{234}Th transport can be important in coastal regions, especially in bays, where large horizontal gradients in ^{234}Th scavenging can occur [18-20].

3. RESULTS AND DISCUSSION

Activity concentrations of dissolved ^{238}U in seawater as well as total ^{234}Th activities in samples collected at the Bransfield Strait both surface and deep waters (Stations 01 to 10 vertical profiles) are shown in Tables 1-10. The 1-D steady-state model described above in equation 1 was used to derive particulate ^{234}Th fluxes exported in the water column. Upper ocean particulate organic carbon export was estimated using modeled ^{234}Th export and the ratio of particulate organic carbon to ^{234}Th on GF/F filters. These data are also presented in Tables 1-10. It can be observed that total ^{234}Th activities in seawater samples studied along the Bransfield Strait ranged from 410 dpm m^{-3} (at Station 06, 299 m depth) to 3240 dpm m^{-3} (Station 01, 25 m depth). Activity concentrations of ^{238}U dissolved in seawater varied from 2350 dpm m^{-3} to 2380 dpm m^{-3}. Activity ratios ^{234}Th total/ ^{238}U above unit were determined at Stations 01, 09 and 10. Non-conservative increases of total ^{234}Th activities related to ^{238}U dissolved (resulting in AR > 1.0) can be representative of several processes, among them:

Table 1. Fluxes of ^{234}Th exported in the particulate (dpm m^{-2} d^{-1}) and the respective POC exported fluxes (mmol C m^{-2} d^{-1}) determined at Station 01.

Depth (m)	$^{238}U_{dis.}$ (dpm m^{-3})	Total ^{234}Th (dpm m^{-3})	P flux (dpm m^{-2} d^{-1})	POC (mmol C L^{-1})	$^{234}Th_{part.}$ (dpm L^{-1})	POC/^{234}Th (mmol C dpm^{-1})	POC flux (mmol C m^{-2} d^{-1})
4	2360	2570	-24,2	0.11	-0.21	0.04	0[b]
25	2360	3240	-532,2	1.65	-0.88	0.51	0[b]
51	2360	2970	-456,8	1.45	-0.61	0.49	0[b]
75	2370	890	1023	0.87	1.48	0.97	995
301	2370	1730	4166	1.13	0.64	0.65	2726
502	2380	2170	1216	1.48	0.21	0.68	831
1000	2380	1970	5880	0.93	0.41	0.47	2776
1498	2380	2090	4159	1.08	0.29	0.52	2147
1993	2380	1940	6273	0.84	0.44	0.43	2714
2205	2380	1670	4335	0.27	0.71	0.16	711

[a] Calculations assumed the hypothesis of a steady-state 1-D model to derive particulate ^{234}Th fluxes. [b] In those cases where particulate ^{234}Th fluxes yield < 0, they were set to zero to perform the assessment of POC exported fluxes.

Table 2. Fluxes of ^{234}Th exported in the particulate (dpm m^{-2} d^{-1}) and the respective POC exported fluxes (mmol C m^{-2} d^{-1}) determined at Station 02.

Depth (m)	$^{238}U_{dis.}$ (dpm m^{-3})	Total ^{234}Th (dpm m^{-3})	P flux (dpm m^{-2} d^{-1})	POC (mmol C L^{-1})	$^{234}Th_{part.}$ (dpm L^{-1})	POC/^{234}Th (mmol C dpm^{-1})	POC flux (mmol C m^{-2} d^{-1})
10	2360	950	406	1.89	1.41	1.99	809
25	2360	1640	311	0.04	0.72	0.02	7.26
25	2360	1800	0	0	0.56	0	0
50	2370	1650	518	0.03	0.72	0.02	10.5
75	2380	1670	511	0.03	0.71	0.02	8.67
105	2360	2040	277	0.03	0.32	0.02	4.63
128	2370	1740	417	0.19	0.63	0.11	45.7
156	2370	720	1331	0.82	1.65	1.14	1516
203	2370	1800	772	1.57	0.57	0.87	673
301	2370	1640	2060	1.24	0.73	0.76	1563
507	2380	1700	4034	0.17	0.68	0.10	411

[a] Calculations assumed the hypothesis of a steady-state 1-D model to derive particulate ^{234}Th fluxes. [b] In those cases where particulate ^{234}Th fluxes yield < 0, they were set to zero to perform the assessment of POC exported fluxes.

Table 3. Fluxes of ^{234}Th exported in the particulate (dpm m^{-2} d^{-1}) and the respective POC exported fluxes (mmol C m^{-2} d^{-1}) determined at Station 03.

Depth (m)	$^{238}U_{dis.}$ (dpm m^{-3})	Total ^{234}Th (dpm m^{-3})	P flux (dpm m^{-2} d^{-1})	POC (mmol C L^{-1})	$^{234}Th_{part.}$ (dpm L^{-1})	POC/^{234}Th (mmol C dpm^{-1})	POC flux (mmol C m^{-2} d^{-1})
10	2360	1790	164	ND	0.57	ND	ND
26	2360	1170	548	ND	1.19	ND	ND
52	2360	1480	659	ND	0.88	ND	ND
74	2360	1850	323	ND	0.51	ND	ND
103	2360	1850	426	ND	0.51	ND	ND
103	2360	1830	0	ND	0.53	ND	ND
200	2370	1380	2766	ND	0.99	ND	ND
301	2380	2060	931	ND	0.32	ND	ND
501	2380	1820	3226	ND	0.56	ND	ND
798	2380	1290	9323	ND	1.09	ND	ND
999	2380	1420	5557	ND	0.96	ND	ND

[a] Calculations assumed the hypothesis of a steady-state 1-D model to derive particulate ^{234}Th fluxes. [b] In those cases where particulate ^{234}Th fluxes yield < 0, they were set to zero to perform the assessment of POC exported fluxes. ND= not determined.

Table 4. Fluxes of ^{234}Th exported in the particulate (dpm m^{-2} d^{-1}) and the respective POC exported fluxes (mmol C m^{-2} d^{-1}) determined at Station 04.

Depth (m)	$^{238}U_{dis.}$ (dpm m^{-3})	Total ^{234}Th (dpm m^{-3})	P flux (dpm m^{-2} d^{-1})	POC (mmol C L^{-1})	$^{234}Th_{part.}$ (dpm L^{-1})	POC/^{234}Th (mmol C dpm^{-1})	POC flux (mmol C m^{-2} d^{-1})
5	2350	1050	187	2.21	1.30	2.11	394
10	2350	2090	37.4	2.18	0.26	1.04	39
25	2350	1900	194	0.02	0.45	0.01	2.56
52	2350	1500	661	0.05	0.85	0.03	22.0
79	2360	2110	194	0.12	0.25	0.06	11.5
100	2370	2320	30.2	1.24	0.05	0.54	16.2
207	2380	2000	1171	1.15	0.38	0.58	676
304	2380	1100	3576	1.56	1.28	1.42	5077
500	2380	1350	5814	1.49	1.03	1.10	6404
795	2380	2110	2294	1.60	0.27	0.76	1737
996	2380	1930	2605	1.64	0.45	0.85	2220

[a] Calculations assumed the hypothesis of a steady-state 1-D model to derive particulate ^{234}Th fluxes. [b] In those cases where particulate ^{234}Th fluxes yield < 0, they were set to zero to perform the assessment of POC exported fluxes.

Table 5. Fluxes of ^{234}Th exported in the particulate (dpm m^{-2} d^{-1}) and the respective POC exported fluxes (mmol C m^{-2} d^{-1}) determined at Station 05.

Depth (m)	$^{238}U_{dis.}$ (dpm m^{-3})	Total ^{234}Th (dpm m^{-3})	P flux (dpm m^{-2} d^{-1})	POC (mmol C L^{-1})	$^{234}Th_{part.}$ (dpm L^{-1})	POC/^{234}Th (mmol C dpm^{-1})	POC flux (mmol C m^{-2} d^{-1})
5	2360	1150	174	1.00	1.21	0.87	151
10	2360	1520	121	1.63	0.84	1.08	130
25	2360	1620	320	1.46	0.74	0.90	288
50	2360	1920	317	1.75	0.44	0.91	289
75	2360	1450	655	1.24	0.91	0.85	559
100	2370	1700	482	0.92	0.67	0.54	261
120	2370	1630	426	1.32	0.74	0.81	345
152	2380	1890	452	0	0.49	0	0
200	2380	1870	705	0	0.51	0	0
302	2380	1540	2468	0.95	0.84	0.62	1525
503	2380	2260	695	1.07	0.12	0.47	330

[a] Calculations assumed the hypothesis of a steady-state 1-D model to derive particulate ^{234}Th fluxes. [b] In those cases where particulate ^{234}Th fluxes yield < 0, they were set to zero to perform the assessment of POC exported fluxes.

Table 6. Fluxes of ^{234}Th exported in the particulate (dpm m^{-2} d^{-1}) and the respective POC exported fluxes (mmol C m^{-2} d^{-1}) determined at Station 06.

Depth (m)	$^{238}U_{dis.}$ (dpm m^{-3})	Total ^{234}Th (dpm m^{-3})	P flux (dpm m^{-2} d^{-1})	POC (mmol C L^{-1})	$^{234}Th_{part.}$ (dpm L^{-1})	POC/^{234}Th (mmol C dpm^{-1})	POC flux (mmol C m^{-2} d^{-1})
5	2360	1650	102	1.46	0.71	0.88	90.3
10	2360	1870	70.6	0.29	0.49	0.16	11.1
25	2360	1470	385	0.07	0.89	0.05	19.4
50	2360	1950	295	0.02	0.41	0.01	3.66
78	2360	1930	347	0.02	0.43	0.01	3.44
102	2370	610	1217	0.02	1.76	0.03	36.5
128	2370	2210	120	0.02	0.16	0.01	1.13
153	2370	1070	936	3.07	1.30	2.87	2690
200	2380	1480	1218	1.74	0.90	1.17	1431
299	2380	410	5617	0.35	1.97	0.86	4825

[a] Calculations assumed the hypothesis of a steady-state 1-D model to derive particulate ^{234}Th fluxes. [b] In those cases where particulate ^{234}Th fluxes yield < 0, they were set to zero to perform the assessment of POC exported fluxes.

Table 7. Fluxes of ^{234}Th exported in the particulate (dpm m^{-2} d^{-1}) and the respective POC exported fluxes (mmol C m^{-2} d^{-1}) determined at Station 07.

Depth (m)	$^{238}U_{dis.}$ (dpm m^{-3})	Total ^{234}Th (dpm m^{-3})	P flux (dpm m^{-2} d^{-1})	POC (mmol C L^{-1})	$^{234}Th_{part.}$ (dpm L^{-1})	POC/^{234}Th (mmol C dpm^{-1})	POC flux (mmol C m^{-2} d^{-1})
5	2350	1880	67.7	1.54	0.47	0.82	55.5
10	2350	1950	57.6	0.38	0.40	0.20	11.3
25	2350	610	752	1.04	1.74	1.70	1276
50	2350	1130	878	0.33	1.22	0.29	254
75	2360	750	1159	0.91	1.61	1.21	1399
100	2370	1110	907	0.37	1.26	0.33	302
150	2370	2000	533	0.03	0.37	0.01	7.10
200	2370	1110	1814	1.70	1.26	1.53	2774
300	2380	1670	2045	0.99	0.71	0.59	1214
500	2380	1140	7142	2.18	1.24	1.91	13667
800	2380	2350	259	1.45	0.03	0.62	161

[a] Calculations assumed the hypothesis of a steady-state 1-D model to derive particulate ^{234}Th fluxes. [b] In those cases where particulate ^{234}Th fluxes yield < 0, they were set to zero to perform the assessment of POC exported fluxes.

Table 8. Fluxes of ^{234}Th exported in the particulate (dpm m^{-2} d^{-1}) and the respective POC exported fluxes (mmol C m^{-2} d^{-1}) determined at Station 08.

Depth (m)	$^{238}U_{dis.}$ (dpm m^{-3})	Total ^{234}Th (dpm m^{-3})	P flux (dpm m^{-2} d^{-1})	POC (mmol C L^{-1})	$^{234}Th_{part.}$ (dpm L^{-1})	POC/^{234}Th (mmol C dpm^{-1})	POC flux (mmol C m^{-2} d^{-1})
5	2360	2130	33.1	0.04	0.23	0.02	0.61
10	2360	1670	99.4	0.02	0.69	0.01	1.24
25	2370	1330	449	2.61	1.04	1.96	881
51	2370	1660	532	1.61	0.71	0.97	515
76	2370	1340	742	1.36	1.03	1.02	754
76	2370	1210	0	0	1.16	0	0
100	2370	2360	6.90	1.22	0.01	0.52	3.56
125	2370	1760	439	0.27	0.61	0.16	69
151	2380	1880	374	0.02	0.50	0.01	4.48
200	2380	1740	903	0.03	0.64	0.02	14.6

[a] Calculations assumed the hypothesis of a steady-state 1-D model to derive particulate ^{234}Th fluxes. [b] In those cases where particulate ^{234}Th fluxes yield < 0, they were set to zero to perform the assessment of POC exported fluxes.

Table 9. Fluxes of ^{234}Th exported in the particulate (dpm m^{-2} d^{-1}) and the respective POC exported fluxes (mmol C m^{-2} d^{-1}) determined at Station 09.

Depth (m)	$^{238}U_{dis.}$ (dpm m^{-3})	Total ^{234}Th (dpm m^{-3})	P flux (dpm m^{-2} d^{-1})	POC (mmol C L^{-1})	$^{234}Th_{part.}$ (dpm L^{-1})	POC/^{234}Th (mmol C dpm^{-1})	POC flux (mmol C m^{-2} d^{-1})
5	2350	3130	-112	73.3	-0.78	23.4	0[b]
10	2350	2400	-7.20	278	-0.05	116	0[b]
25	2350	2020	143	240	0.33	119	16963
50	2350	2120	166	20.0	0.23	9.45	1565
74	2360	2720	-249	4.45	-0.36	1.64	0[b]
100	2370	1570	599	13.4	0.80	8.51	5095
200	2380	2810	-1238	0	-0.43	0	0[b]
303	2380	2130	742	0	0.25	0	0.87
501	2380	2140	1369	0	0.24	0	1.60
794	2380	570	15274	0	1.81	0	66.9
1000	2380	1230	6823	0	1.15	0	13.9

[a] Calculations assumed the hypothesis of a steady-state 1-D model to derive particulate ^{234}Th fluxes. [b] In those cases where particulate ^{234}Th fluxes yield < 0, they were set to zero to perform the assessment of POC exported fluxes.

Table 10. Fluxes of ^{234}Th exported in the particulate (dpm m^{-2} d^{-1}) and the respective POC exported fluxes (mmol C m^{-2} d^{-1}) determined at Station 10.

Depth (m)	$^{238}U_{dis.}$ (dpm m^{-3})	Total ^{234}Th (dpm m^{-3})	P flux (dpm m^{-2} d^{-1})	POC (mmol C L^{-1})	$^{234}Th_{part.}$ (dpm L^{-1})	POC/^{234}Th (mmol C dpm^{-1})	POC flux (mmol C m^{-2} d^{-1})
6	2360	2400	-6.90	0.79	-0.04	0.33	0[b]
9	2360	1370	85.5	1.14	0.99	0.83	71.1
24	2360	1400	415	0.15	0.96	0.11	45.6
52	2360	1420	758	1.73	0.94	1.22	925
75	2360	1840	344	0	0.52	0	0
100	2360	2260	72.0	1.54	0.10	0.68	48.9
125	2370	2010	259	0.90	0.36	0.45	117
151	2370	1880	367	1.51	0.49	0.80	294
201	2380	1770	878	1.03	0.61	0.58	513
301	2380	1590	2275	1.68	0.79	1.06	2404
499	2380	1210	6672	1.02	1.17	0.85	5651

[a] Calculations assumed the hypothesis of a steady-state 1-D model to derive particulate ^{234}Th fluxes. [b] In those cases where particulate ^{234}Th fluxes yield < 0, they were set to zero to perform the assessment of POC exported fluxes.

(a) lower resolution of total ^{234}Th vertical profiles; (b) processes of re-suspension and/or upwelling; (c) other sources of ^{234}Th to the studied system, for example, those related to the ice melting and runoff. Recent findings for three species of Antartic crustaceans have suggested that under certain conditions krill-associated ^{234}Th would generate a several-fold positive export bias in depth-integrated ^{234}Th profiles [21]. These results, coupled with published values of krill densities as high as 100 g L^{-1}, which commonly occur in the Southern Ocean suggest that ^{234}Th bioaccumulation could result in up to 90% of total water-column ^{234}Th being associated with krill. Hence, the occurrence of a synchronized molting event [22] within a high-biomass krill school could cause the ^{234}Th distribution in the water column to be almost entirely a result of radionuclide uptake by these organisms and consequently bias the results of traditional ^{234}Th based models by more than one order of magnitude. Activity ratios of total ^{234}Th/^{238}U close to 1.0 indicate lower fluxes of particulate exported, while values around 0.6 in the euphotic zone suggest higher fluxes. However, it was noticed a spatial variability between vertical profiles established and unfortunately, due to a single sampling program, no comparison regarding seasonality could be performed. Almost all ^{234}Th vertical profiles showed layers of increased activities below the chlorophyll–a maximum values, associated to processes of particle remineralization and resulting in decreased fluxes at these water column depths.

The radioactive equilibrium between total ^{234}Th and ^{238}U was observed around 500 m depth at Stations 01 and 05. In the cases of Stations 02, 06, 08 and 10, the radioactive equilibrium occurred at water depth of 100 m. If we consider vertical profiles obtained for Stations 04 and 07, we can verify that the equilibrium condition can be reached both at 100 m depth and 800 m depth. At Station 03, the equilibrium was observed at 301 m. The radioactive equilibrium was not detected at Station 09.

In all vertical profiles studied in this research work, the particulate organic matter percentual in the total suspended matter was below than 50 %, except in Station 05, where between 50 and 200 m depth the particulate organic matter represented more than 80% of the total suspended material. Besides that, vertical profiles of total ^{234}Th, particulate organic matter and suspended matter showed similar distributions, mainly below 200 m water depth.

Regarding nutrient distributions, phosphate concentrations ranged from 0.44 µmol $L^{-1}$to 2.75 µmol L^{-1}, with increased values being observed at Station 02, at 75 m depth. Staions 08, 09 and 10 showed low concentrations of phosphate, while Station 04 presented levels higher than 2.0 µmol L^{-1}. Station 01 presented the highest nitrate values, varying from 43.85 µmol L^{-1} to 51.49 µmol L^{-1}. At Station 02, it was also observed increased concentrations of nitrate below 156 m depth, revealing the formation of Antartic Deep Water, enriched in inorganic nitrogen compounds. The highest silicate concentration was determined at Station 01 (1993 m depth). Increased silicate values were also measured in deep water from Stations 01, 02, 05, 07 and 08. These results indicate a combination of erosional continental input, ice melting and the formation of deep waters enriched in nutrients. Chloropyll-a distributions showed increased concentrations between 10 and 75 m depth interval, and demonstrated the phytoplankton *bloom* typical of austral summer. Station 08 is the closest of the Antartic Peninsula and presented total ^{234}Th activities in equilibrium with ^{238}U at the surface, besides high silicate values, supported by freshwater input. In the case of ^{234}Th, fluxes tended to be largest nearshore and decreased with increasing distance from land, indicating the importance of the coast on ^{234}Th activity distributions. ^{234}Th particulate fluxes exported up to 15274 dmp m^{-2} d^{-1} were estimated, the highest value observed in Station 09 at 794 m depth. POC

exported fluxes derived from the disequilibrium $^{234}Th/ ^{238}U$ model varied from 0.6 to 16000 mmol C m^{-2} d^{-1}.

4. CONCLUSIONS

Understanding the mechanisms that regulate carbon export from oceanic surface waters to depth remains a critical gap in global ocean carbon geochemistry. The oceanic reservoir contains about 60 times more CO_2 than the atmosphere. Moreover, the surface ocean and atmospheric CO_2 levels are lower than expected in comparison to deep oceanic CO_2 concentrations. This discrepancy is caused by the photosynthetic uptake of CO_2 and its removal to deep ocean as the remains of phytoplankton sink below the euphotic zone (biological pump). There is a general agreement that changes in the efficiency of the "biological pump" can and might have drastically altered global climate by changing atmospheric CO_2 concentrations. The Southern Ocean has the potential to influence climate due to its large inventory of excess macronutrients such as nitrate and phosphate.

In this research work, a combination of natural radionuclides were used to examine particle scavenging, removal and surface water mixing rates in order to evaluate the potential influence of ice melting on the production and export of particulate organic carbon. The ability to accurately model biogeochemical cycles of carbon, nitrogen and other nutrients relies on how well the distributions and behaviors of the factors limiting primary production are understood. The magnitude of upper ocean particulate organic carbon export was assessed by quantifying total ^{234}Th deficits with respect to its conservative parent nuclide ^{238}U in seawater. This proxy was proven to be useful to trace oceanic biogeochemical processes occurring over timescales of days to weeks. Total ^{234}Th activities in seawater samples studied along the Bransfield Strait ranged from 410 dpm m^{-3} (at Station 06, 299 m depth) to 3240 dpm m^{-3} (Station 01, 25 m depth). Activity concentrations of ^{238}U dissolved in seawater varied from 2350 dpm m^{-3} to 2380 dpm m^{-3}. Activity ratios ^{234}Th total/ ^{238}U above unit were determined at Stations 01, 09 and 10. Non-conservative increases of total ^{234}Th activities related to ^{238}U dissolved (resulting in AR > 1.0) were related to process associated to ice melting, freshwater runoff and biomass bioaccumulation. Activity ratios of total $^{234}Th/^{238}U$ close to 1.0 indicate lower fluxes of particulate exported, while values around 0.6 in the euphotic zone suggest higher fluxes. Spatial variability between vertical profiles established was observed and since these data reflects a single sampling program, no comparison regarding seasonality could be performed. ^{234}Th particulate fluxes exported up to 15274 dmp m^{-2} d^{-1} were estimated, the highest value observed in Station 09 at 794 m depth. POC exported fluxes derived from the disequilibrium $^{234}Th/ ^{238}U$ model varied from 0.6 to 16000 mmol C m^{-2} d^{-1}.

ACKNOWLEDGMENTS

This experiment involved many collaborators, without whom this study would not have been possible. In particular, we thank the scientists and crews aboard the RV Ary Rongel (Brazilian Navy) for their help and assistance. Science support was provided by CNPq – PROANTAR Project n˚ 550048/2007-3.

REFERENCES

1. P.W. Boyd, A.J. Watson, C.S. Law, E.R. Abraham, T. Trull, R. Murdoch, D.C.E. Bakker, A.R. Bowie, K.O. Buesseler, H. Chang, M. Charette, P. Croot, K. Downing, R. Frew, M. Gall, M. Hadfield, J. Hall, M. Harvey, G. Jameson, J. LaRoche, M. Liddicoat, R. Ling, M.T. Maldonado, R.M. Mckay, S. Nodder, S. Pickmere, R. Pridmore, S. Rintoul, K. Safi, P. Sutton, R. Strzepek, K. Tanneberger, S. Turner, A. Waite, J. Zeldis. "A mesoscale phytoplancton bloom in the polar Southern Ocean stimulated by iron fertilization", *Nature,* **407(6805):** pp. 695-702 (2000).
2. K.O. Buesseler, R.T. Barber, M.L. Dickson, M.R. Hiscock, J.K. Moore, R. Sambrotto, "The effect of marginal ice-edge dynamics on production and export in the Southern Ocean along 170◦W", *Deep Sea Research Part II: Topical Studies in Oceanography,* **50(3-4):** pp. 579-603 (2003).
3. O. Holm-Hansen. "Nutrient cycles in Antartic marine ecosystems". In Siegfried, W.R., Condy, P.R., Laws, R.M. (eds), *Antartic nutrient cycles and food webs:* 6-10. Berlim, Heidelberg, Springer-Verlag.
4. O. Holm-Hansen, A.F. Amos, N. Silva, V.E. Villafañe, E.W. Helbling, E.W. "In situ evidence for a nutrient limitation of phytoplankton growth in pelagic Antartic waters", *Antartic Science,* **6(3):** pp. 315-324 (1994).
5. D.A. Hutchins, K.W. Bruland. "Iron-limited diatom growth and Si:N uptake ratios in a coastal upwelling regime", *Nature,* **393(6685):** pp. 561-564 (1998).
6. J.K. Cochran, P. Masqué. "Short-lived U/Th-series radionuclides in the oceans: tracers for scavenging rates, export fluxes and particle dynamics", *Rev. Mineral Geochem,* **52:** pp. 461-492 (2003).
7. M. Zhou, P.P. Niiler, Y. Zhu, R.D. Dorland. "The western boundary current in the Bransfield Strait, Antartica", *Deep-Sea Research I,* **53:** pp. 1244-1252 (2006).
8. K.O. Buesseler, C. Benitez-Nelson, M. Rutgers van der Loeff, J. Andrews, L. Ball, G. Grossin, M.A. Charette. "An intercomparison of small and large volume techniques for thorium-234 in seawater", *Marine Chemistry,* **74:** pp. 15-28 (2001).
9. G. Cutter, P. Andersson, L. Codispoti, P. Croot, R. François, M. Lohan, H. Obata, M. Rutgers van der Loeff. "Sampling and sample-handling protocols for Geotraces-related IPY Cruises 2007-2008", prepared by the Geotraces standards and intercalibration committee, pp.1-32 (2010).
10. J.D.H. Strickland, T.R. Parsons. "A practical handbook of seawater analysis", *Fisheries Research Board of Canada Bulletin,* **157,** Otawa (1972).
11. K. Grasshoff, K. Kremling, M. Ehrhardt. *Methods of Seawater Analysis.* 3rd ed. Wiley-Vch, Weinheim, Federal Republic of Germany (1998).
12. P. Tréguer, P. Lê Corre, P. *A manuel d' analysis des sels nutrifs dans l'eau de mer.* 2ème ed. Brest: Université de Bretagne Occidentale. 110p. (1975).
13. K.C.S. Almeida, H. Oikawa, J. Oliveira, C.L. Duarte. "Degradation of petroleum hydrocarbons in seawater by ionizing radiation", *Journal of Radioanalytical and Nuclear Chemistry,* **270 (1):** pp. 93-97 (2006).
14. J.H. Chen, R.L. Edwards, G.J. Wasserburg. "^{238}U, ^{234}U and ^{232}Th in seawater", *Earth and Planetary Science Letters,* **80:** pp. 242-251 (1986).
15. K.O. Buesseler, M.P. Bacon, J.K. Cochran, H.D. Livingston. "Carbon and nitrogen export during JGOFS North Atlantic Bloom Experiment estimated from ^{234}Th:^{238}U disequilibria", *Deep-Sea Research,* **39:** pp. 1115-1137 (1992).

16. K.O. Buesseler. “The decoupling of production and particle export in the surface ocean”, *Glob. Biogeochem. Cycles*, **12:** pp. 297-310 (1998).
17. K.O. Buesseler, J.A. Andrews, M.C. Hartman, R. Belastock, F. Chai. “Regional estimates of the export flux of particulate organic carbon derived from Th-234 during JGOFS EQPAC program”, *Deep-Sea Research II*, **42:** pp. 777-804 (1995).
18. J.K. Cochran, C. Barnes, D. Achman. “Thorium-234/Uranium-238 disequilibrium as an indicator of scavenging rates and particulate organic carbon fluxes in the northeast polynya, Greenland”, *Journal of Geophysical Research*, **100:** pp. 4399-4410 (1995).
19. S.B. Moran, K.O. Buesseler. “Size-Fractionated ^{234}Th in Continental Shelf Waters off New England: Implications for the Role of Colloids in Oceanic Trace Metal Scavenging”, *Journal of Marine Research*, **51:** pp. 893-922 (1993).
20. O. Gustafsson, K.O. Buesseler, W.R. Geyer, S.B. Moran, P.M. Gschwend. “An assessment of the relative importance of horizontal and vertical transport of particle-reactive chemicals in the coastal ocean: two-dimensional Th-234 modeling”, *Continental Shelf Research*, **18:** pp. 805-829 (1998).
21. A.M. Rodriguez y Baena, M. Metian, J.L. Teyssié, C. De Broyer, M. Warnau. “Experimental evidence for ^{234}Th bioaccumulation in three Antartic crustaceans: potential implications in particle flux studies”, *Marine Chemistry*, **100:** pp. 354-365 (2006).
22. W.M. Hamner, P.P. Hamner, S.W. Strand, R.W. Gilmer. “Behavior of Antartic krill, *Euphausia superba*; chemoreception, feeding, schooling, and molting”, *Science*, **220:** pp. 433-435 (1983).